Renewable Energy and Power Quality Journal
https://repqj.com/index.php/repqj/index
RE&PQJ, Vol. 23, No. 1, 2025

Automatic Switching Strategy of Grid-Connected/Off-Grid Mode of Photovoltaic Storage and Charging Integrated Station Based on Intelligent Control

Han Fu*, Xiaoyu Liu, Xiaoming Chen, Yuanqi Ni, Hong Zheng

State Grid Hubei Electric Power Co., Ltd. Wuhan Power Supply Company, Wuhan 430010, Hubei, China
*Corresponding author's email: fu76203915@126.com

Abstract. With the widespread application of renewable energy, photovoltaic (PV) storage and charging (SC) integrated stations are important in providing a stable power supply and optimizing energy management. Traditional integrated PV SC stations mostly use the PID (Proportion Integral Differential) control algorithm for automatic switching in grid-connected/off-grid (GC/OG) mode. The switching decision accuracy is low, energy consumption is increased, and there needs to be a more intelligent prediction of future photovoltaic power generation (PVPG), load demand and grid conditions. This paper is the first to combine the advantages of the dynamic decision-making of the DQN (Deep Q-Network) algorithm and the time series prediction of the LSTM (Long Short-Term Memory) model to study the automatic switching strategy of the grid-connected/off-grid mode of the integrated photovoltaic storage and charging station. The study first built a PV SC integrated station model, including PVPG, energy storage system, power grid model and load demand model, and set the objective function and constraints. Then, the LSTM model was used to predict the future load demand and PVPG of the PV SC integrated station, and the prediction was input into the DQN model. Finally, the DQN model combined the LSTM prediction results with the current environmental status to decide whether the PV SC integrated station should be connected to or off the grid. The experiment is based on the data of the PV SC integrated station actually deployed in a particular area from January to June 2023, and the performance of the GC/OG mode automatic switching strategy of the PV SC integrated station is statistically analyzed. The experimental results show that the strategy switching accuracy of the DQN-LSTM (Deep Q-Network-Long Short-Term Memory) model reaches 95.87%, which is 15.44% higher than the traditional PID, and the energy efficiency ratio is as high as 1.75. The experimental results show that the DQN-LSTM model combined with intelligent control can automatically switch the GC/OG mode of the integrated PV SC station, which significantly improves the accuracy and efficiency of the strategy and reduces energy consumption to a certain extent.

Key words. Photovoltaic storage and charging integrated station, grid-connected/off-grid mode, intelligent control, DQN-LSTM model, Switching accuracy

1. Introduction

As the global demand for sustainable energy increases, PVPG has been widely used as a green and clean energy form [1,2]. To improve energy efficiency and reduce dependence on the power grid, integrated PV SC stations have become a solution that has attracted much attention in recent years [3-5]. How to efficiently achieve GC/OG mode switching and ensure system stability and optimal energy efficiency is still a hot and challenging issue in current research.

In recent years, with the integration of PVPG, energy storage systems and charging piles in photovoltaic energy storage integrated stations, many scholars have begun to study the GC/OG mode automatic switching problem and have achieved many research results. Yao M, Wu K Y, and other scholars reviewed the capacity allocation, energy management and control strategies of photovoltaic energy storage integrated electric vehicle charging stations, providing an important research basis for this paper [6,7]. Hmad J and other scholars used microgrid technology to convert the grid-connected and off-grid modes, ensuring a smooth transition between the grid-connected and off-grid modes [8]. Based on the adaptive fuzzy neural reasoning system and adaptive fuzzy PID control, the NMC (nonlinear multimode controller) controller has been widely used in the switching of photovoltaic-WT (Wind Turbine) system grid-connected and off-grid and energy storage inverter seamless off-grid, significantly reducing the switching time [9-11]. Kampik M et al. constructed a threshold-based converter system for switching between off-grid and grid-connected operation modes, which improved the switching efficiency, but it could not adapt to dynamic and complex environments [12]. Perumal V et al. used a controller developed using the MPSO (modified particle swarm optimization) algorithm to

switch the grid mode, achieving fast and smooth switching of the grid mode [13]. The above scholars use PID control, threshold-based controllers, etc., to analyze historical data and achieve flexible mode switching. However, these methods have poor switching decision accuracy and need long-term prediction of future load demand and PVPG, making it difficult to cope with dynamic changes in complex environments.

To overcome the low switching decision accuracy and lack of intelligent prediction capabilities, many scholars have begun to explore dynamic decision-making methods based on intelligent control and have achieved good results. Among them, applying deep reinforcement learning and time series prediction models in energy management has achieved certain breakthroughs. As a type of reinforcement learning, the DDQN (Double Deep Q-Network) algorithm has been widely used in the cost-effective operation of residential buildings with grid-connected photovoltaic battery systems, significantly reducing costs [14,15]. The TD3 (Twin Delayed Deep Deterministic policy gradient) algorithm has been well applied in the management of grid-connected wind-microturbine-photovoltaic-electric vehicle energy systems and grid-connected photovoltaic systems, improving the switching efficiency between grid-connected and off-grid systems while reducing costs [16,17]. Qi J et al. used the DQN algorithm to dispatch microgrids and improve dispatch efficiency optimally [18]. Mohammad F et al. introduced a fusion model of ConvLSTM (Convolutional Long Short-Term Memory) and BiConvLSTM (Bidirectional Convolutional Long Short-Term Memory) to predict the network energy demand load of electric vehicle charging stations, achieving good prediction results and providing a basis for strategy advancement for subsequent intelligent decision-making [19]. Yang C, Aduama P and other scholars used LSTM model to predict the load of electric vehicle charging stations, achieving extremely low prediction error [20,21]. Avar et al. used bidirectional LSTM to predict photovoltaic power generation and load demand, reducing deviation and improving efficiency [22]. The above scholars used TD3 algorithm, DQN algorithm and other algorithms to make decisions and control grid-connected photovoltaic cells and other energy systems, achieving good results. However, there are few studies on applying deep intensity learning models in the automatic switching of GC/OG mode in integrated PV SC stations, and scholars have not been able to integrate intelligent strategies and future load forecasting.

This study aims to address the decision-making accuracy and energy efficiency issues faced by integrated PV SC stations in GC/OG mode switching. It adopts an intelligent decision-making strategy based on deep reinforcement learning and time series prediction. In the experiment, a comprehensive model of the integrated PV SC station is built first, covering multiple factors such as PVPG, energy storage system, power grid and load demand, ensuring the comprehensiveness and practical operability of the system model. LSTM is used to make time series predictions for future load demand and PVPG, and the prediction results are input into the DQN model. The DQN model then uses the real-time environmental status and the LSTM prediction results to jointly decide whether to switch to grid-connected or off-grid mode, thus optimizing the decision-making process. Through a series of experiments based on actual data, the study verifies the significant advantages of the DQN-LSTM model in improving the GC/OG mode switching accuracy, energy efficiency ratio and system response speed of the integrated PV SC station. The experimental results show that DQN-LSTM significantly improves the accuracy and efficiency of strategy switching and also effectively improves the overall performance of energy management, demonstrating its potential application in renewable energy management.

Contribution of the paper:

(1) This paper innovatively combines the DQN algorithm with the LSTM model, fully utilizing deep reinforcement learning's dynamic decision-making ability of deep reinforcement learning and the advantages of LSTM in time series prediction. It also deepens the research depth in GC/OG mode switching of PV SC integrated stations.

(2) The study comprehensively considers multiple key factors such as PVPG, energy storage system, grid conditions and load demand. A comprehensive and practical PV SC integrated station model is also constructed. This model provides accurate input data for decision-making, ensures the algorithm's practical application value, providing a reference for future scholars.

(3) Experimental verification shows that the DQN-LSTM model performs well in improving energy utilization efficiency and significantly improves the system's energy management performance. The optimization decision-making process of the DQN-LSTM model improves the overall economic benefits, showing its wide application potential in renewable energy management and its value in green and low-carbon development.

2. Design of GC/OG Mode Automatic Switching Strategy for Integrated Photovoltaic, Storage and Charging Station

A. Construction of Integrated Photovoltaic, Storage and Charging Station Model

1) PVPG Model

By combining solar PVPG with battery energy storage system, efficient production, storage and distribution of electricity are realized, and charging services are provided for electric vehicles and other equipment [23-25]. In the PVPG model, the output power depends on the light intensity, ambient temperature and the

efficiency of the photovoltaic panel. The modeling expression of the PVPG model is shown in formula (1).

$$p_g(t) = B(t) \cdot I \cdot \alpha_g cos(\theta) (1)$$

$p_g(t)$ represents PVPG.

2) Energy Storage System Model

Battery packs and battery management systems are part of the energy storage system [26,27]. Formula (2) shows the modeling expression of the battery pack charging and discharging process.

$$D(t+1) = D(t) + \frac{P_b(t) \cdot \Delta t}{C_b} (2)$$

3) Load Demand Model

The load demand model covers historical data and future forecast values. The expression of the load demand model is shown in formula (3).

$$E(t) = f(E(t-1), E(t-2), \cdots, E(t-n)) (3)$$

f represents the function of the LSTM model learning historical data and predicting load demand.

4) Grid Model

The expression of the total system power is shown in formula (4).

$$P_{to}(t) = P_g(t) + P_b(t) + P_{gr}(t) (4)$$

5) Energy Management Objective Function and Constraints

The system in the integrated PV SC station aims to maximize energy efficiency and ensure stable power supply [28]. The objective function is expressed as shown in formula (5).

$$\text{Ob} = \max \sum_{t=0}^{T} (\beta P_g(t) + \gamma P_b(t) - \delta P_{gr}(t)) (5)$$

β, γ, and δ represent weight coefficients.

When constructing the PV SC integrated station model, the constraints are as follows:

The constraint of battery charging and discharging restrictions are shown in formula (6).

$$0 \le D(t) \le C_b (6)$$

The constraint corresponding to the power balance are shown in formula (7).

$$P_g(t) + P_b(t) = E(t) + P_{gr}(t) (7)$$

The battery power limit is shown in formula (8).

$$P_b^{max} \ge |P_b(t)| \ge 0 (8)$$

P_b^{max} represents the maximum charge and discharge power of the battery.

The energy management problem of integrated photovoltaic storage and charging stations is a non-convex optimization problem. The problem involves multiple complex constraints, such as battery charging and discharging restrictions, power balance, and battery power restrictions. These constraints make the relationship between the objective function and the constraints nonlinear and have multiple local minima.

To solve this non-convex optimization problem, this paper adopts the DQN algorithm. DQN combines the advantages of deep learning and Q learning. It estimates the state-action value function by training a deep neural network to guide the intelligent agent to make the best decision in a complex and dynamically changing environment. In the energy management problem of integrated photovoltaic storage and charging power stations, DQN can effectively learn the optimal energy scheduling strategy through interaction with the environment. This can achieve the optimal operation of the system in terms of battery charging and discharging, photovoltaic power generation, energy storage and grid interaction, maximize energy efficiency, and ensure power supply stability.

B. DQN Algorithm Construction and Training

1) DQN Algorithm

DQN (deep Q-learning) [29-31] combines the ideas of deep neural networks and Q learning, and uses the approximate representation of the Q-value function to achieve learning and optimization of the action value function in complex environments.

2) DQN Design (State Space, Action Space, Reward Function Design)

(1) State space design

In fully describe the state of the PV SC integrated station, the experiment selects key features related to the power grid, PVPG, energy storage system and load demand,

including PVPG power, charging state of energy storage battery, load demand, grid power, etc. The definition of the state space is shown in formula (9).

$$S(t) = \left[P_g(t), D(t), E(t), P_{gr}(t) \right] (9)$$

$E(t)$ represents the load demand, which corresponds to the user's electricity demand.

(2) Action space design

The action space defines the operation of the DQN algorithm in a given state. DQN makes the most appropriate decision at each time step based on the current state, ensuring that the PV SC integrated station can efficiently switch between grid-connected and off-grid. This paper's action space includes two operation modes: grid-connected and off-grid. The definition of the action space is shown in formula (10).

$$A(t) = \left[a_1, a_2 \right] (10)$$

a_1 represents the off-grid mode, and the corresponding value is 0. a_2 represents the grid-connected mode, and the corresponding value is 1.

(3) Reward function design

As a core part of DQN, the reward function measures the return brought by a certain action. In the automatic switching strategy of the PV SC integrated station, the goal of this paper is to maximize the system's energy efficiency and reduce unnecessary energy consumption. The reward function is designed based on the efficiency of PVPG and energy storage batteries, the degree of grid dependence, and the degree of matching of load demand.

The reward function design expression is shown in formula (11).

$$R(t) = \varepsilon \cdot (P_g(t) - E(t)) - \mu \cdot \left| D(t) - D_t \right| - \rho P_{gr}(t) (11)$$

D_t represents the target battery charge state value, which is 50% of the original value.

The reward function design diagram is shown in Figure 1.

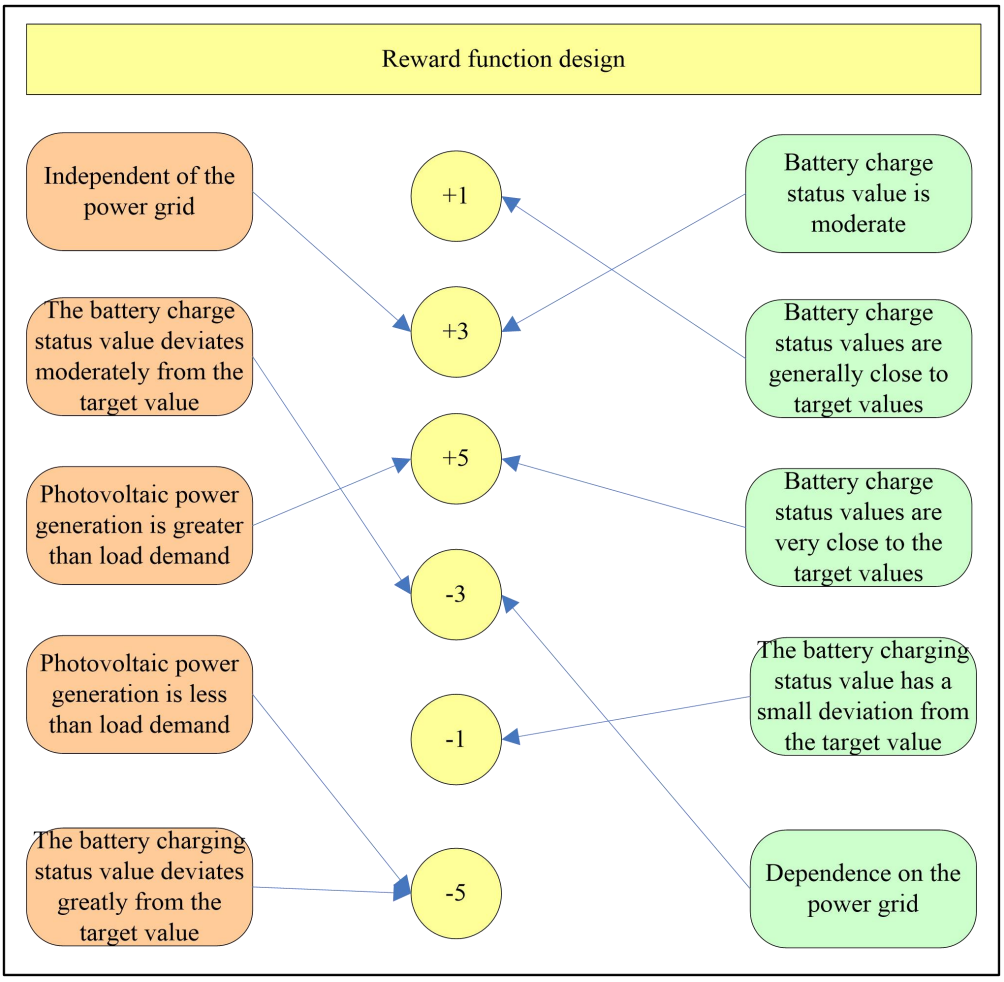

Figure 1. Reward function design diagram

In terms of energy storage system utilization efficiency, when the energy storage battery is fully utilized and the battery charge state value is in a moderate range, the system gets a positive reward of +3. If the target value is very close, it is +5, and if it is generally close to the target value, it is +1. If the battery charging state value is far from the target value, a negative reward is given according to the degree of deviation. If the deviation is large, it is -5, if the deviation is medium, it is -3, and if the deviation is small, it is -1. In terms of the degree of grid dependence, if the system depends on the grid, it corresponds to the grid-connected mode and a negative reward of -3 is given, otherwise it corresponds to the off-grid mode and a positive reward of +3 is given.

3) DQN Algorithm Construction

The DQN algorithm structure constructed in this paper is divided into an input layer, a hidden layer, and an output layer. The input layer is the state of the integrated PV SC station system, and the output layer is the Q value and action corresponding to the action. To improve training efficiency and stability, the DQN algorithm adopts an experience replay mechanism [32,33]. Through experience replay, the intelligent agent can break the time correlation in the training process, reduce the correlation between data, and make the training process more stable.

The steps of the DQN algorithm are as follows:

(1) The parameters of the deep neural network and the target network can be initialized first, and the experience replayer can be initialized.

(2) It can select an action under the current strategy, observe the reward and next state returned by the environment after executing the action, and then store the experience tuple in the experience replay memory.

(3) A small batch of experience tuples can be randomly sampled from the experience replay memory, and the target network can be used to predict the Q value of the next state and calculate the target value.

4) Loss Function and Parameter Update

In DQN training, the loss function is mainly used to measure the difference between the current network output Q value and the target Q value. DQN uses the Q-Learning objective function for update, and the calculation of the loss function is shown in formula (12).

$$L(\theta) = E_{(s,a,r,s)'\sim O}\left[z_t - Q(s_t, a_t; \theta)^2 \right] (12)$$

z_t represents the target Q value, and O represents the experience replay buffer.

The calculation formula for the output target Q value is shown in formula (13).

$$z_t = r + \zeta \max_{a'} Q(s_t', a'; \theta^-) (13)$$

The Adam optimizer combines the gradient descent and momentum methods and can converge quickly in most cases. This paper uses the Adam optimizer to minimize the loss function and update the network parameters as shown in formula (14).

$$\theta_t' = \theta_t - \varphi \cdot \frac{\vartheta_t}{\sqrt{\iota_t} + \kappa} (14)$$

ϑ_t represents the first-order moment estimate, and ι_t represents the second-order moment estimate. κ represents a very small constant, and φ represents the learning rate.

C. LSTM Model Design and Training

In this study, the paper use a standard LSTM neural network for load demand and PV output forecasting, mainly considering the simplicity and interpretability of the model. More complex models such as bidirectional LSTM and stacked LSTM can better capture the long-term and short-term dependencies in time series in some cases, resulting in higher prediction accuracy, but these models are more complex and more difficult to train and tune. To ensure that the model is trained in a reasonable time and has good generalization capabilities, the standard LSTM network is selected for the experiment.

In the GC/OG mode automatic switching strategy of the integrated PV SC station, this paper applieds the LSTM model [34-36] to perform time series prediction of load demand and PVPG. As a deep learning model, the LSTM model can effectively model long-term dependencies, provide accurate predictions for future load demand and power generation, and provide reliable decision input for the DQN algorithm.

The input layer of the LSTM model inputs the load demand and PVPG in the PV SC integrated station in the past n time steps. Then, the LSTM unit layer uses the gating mechanism to selectively remember or forget the information and output the load demand and PVPG forecast value at a certain moment in the future.

Forget gate is shown in formula (15).

$$g_t = \xi(U_f \left[m_{t-1}, \varpi_t \right] + \psi_g) (15)$$

Input gate is shown in formula (16).

$$j_t = \xi(U_j[m_{t-1}, \varpi_t] + \psi_j) \quad (16)$$

Candidate memory cellis shown in formula (17).

$$\tilde{M}_t = tan(U_M[m_{t-1}, \varpi_t] + \psi_M) \quad (17)$$

Memory cell update is shown in formula (18).

$$M_t = g_t \cdot M_{t-1} + j_t \cdot \tilde{M}_t \quad (18)$$

Output gate is shown in formula (19).

$$\Phi_t = \xi(U_\Phi[m_{t-1}, \varpi_t] + \psi_\Phi) \quad (19)$$

Hidden state is shown in formula (20).

$$m_t = \Phi_t \cdot tanh(M_t) \quad (20)$$

D. Fusion of DQN Model and LSTM Model

In this paper, the DQN model and LSTM model are responsible for the tasks of intelligent decision-making and time series prediction respectively. The study uses a cascade structure to fuse the DQN and LSTM models. The LSTM model first performs time series forecasting on PVPG and load demand and uses the forecast results as the input of the DQN model. The DQN model uses learning to obtain the optimal GC/OG decision. The core of the cascade structure fusion method is to enhance DQN's ability to predict future states through the output of LSTM so that it can make more accurate decisions in a dynamically changing environment.

In the DQN-LSTM fusion model, DQN calculates the corresponding Q value based on the current state and prediction results in each training step and updates its network parameters. The prediction value output by LSTM helps DQN better judge the future state and improve the accuracy of decision-making. The training of the LSTM model and the DQN model is synchronized to a certain extent, and the error feedback of the LSTM during the training process affects the parameter update of the DQN through back propagation.

The structure of the DQN-LSTM fusion model is shown in Figure 2.

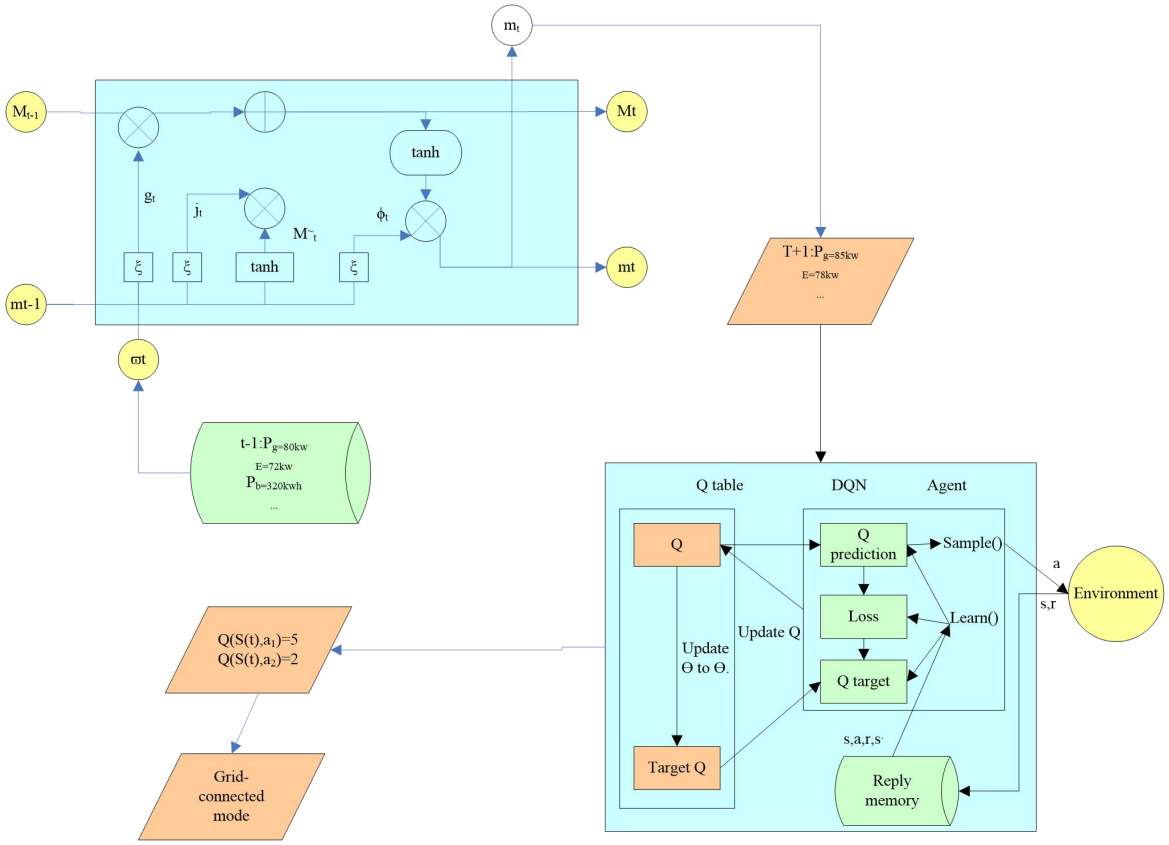

Figure 2. Structure of DQN-LSTM fusion model

E. GC/OG Mode Switching Logic

The DQN model selects the appropriate mode based on the calculated Q value. The switching rules are as follows. When the energy storage battery is fully charged and photovoltaic power generation cannot meet the load demand, the system will prioritizes off-grid mode and provides power through the energy storage battery. When

the energy storage battery is insufficient and the photovoltaic power generation is greater than the load demand, the system will switches to grid-connected mode. The switching conditions between the grid-connected mode and the off-grid mode are shown in formula (21).

$$\begin{aligned} P_b(t) \geq P_{xb} \ and \ P_g(t) \geq E(t) \\ P_b(t) < P_{xb} \ and \ P_g(t) < E(t) \end{aligned} \quad (21)$$

P_{xb} represents the sufficient threshold of the energy battery.

When the energy storage battery power is moderate and the PVPG power is close to the load demand, the system decides to connect to the grid or go off the grid according to the actual situation. When the energy storage battery power and PVPG power are both unstable, the prediction and intelligent decision-making of the DQN model are used to make switching.

The classification tree diagram of various control strategies for the storage system of the renewable energy station is shown in Figure 3. Figure 3 clearly shows the structure and characteristics of various methods, which provides an intuitive reference for understanding and selecting storage system control strategies suitable for different scenarios.

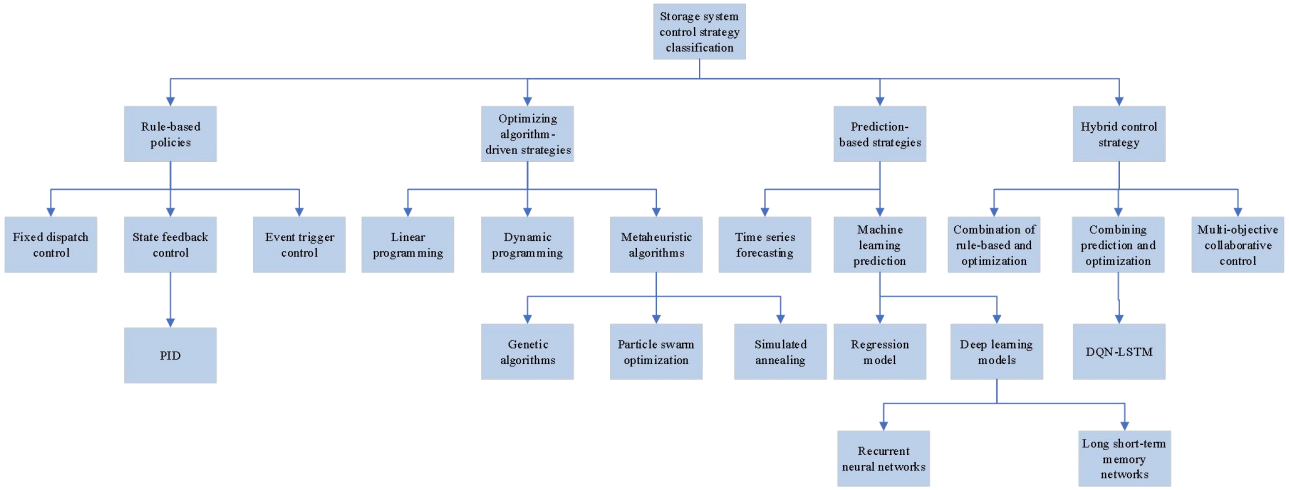

Figure 3. Classification tree of various control strategies for storage systems of renewable energy stations

In Figure 3, a tree flow chart shows the main classification and subclassification of storage system control strategies for renewable energy stations connected to smart grids. The control strategies are divided into four categories: rule-based strategies, optimization algorithm-driven strategies, prediction-based strategies, and hybrid control strategies. Rule-based strategies include simple methods such as fixed scheduling control, state feedback control, and event-triggered control. Optimization algorithm-driven strategies cover linear programming, dynamic programming, and meta-heuristic algorithms such as genetic algorithms and particle swarm optimization. Prediction-based strategies focus on time series analysis and machine learning prediction, among which deep learning methods such as recurrent neural networks and LSTM networks. Hybrid control strategies integrate rules, optimization, and prediction, and propose solutions for multi-objective collaborative control.

3. GC/OG Mode Automatic Switching Strategy Evaluation Experiment

A. Experimental Environment

Hardware environment: Intel Core i9-13900K, NVIDIA RTX 4090, 64 GB DDR5 5600 MHz, 2 TB NVMe SSD.

Software environment: Windows 11 Pro, Python 3.11, PyTorch 2.1.0, Matplotlib 3.8.2, Pandas 2.1.1, CUDA 12.2.

In the construction of the experimental test bench, this paper builds a high-precision experimental platform based on the hardware and software environment. The test bench simulates the actual operation of the photovoltaic power generation system and integrates energy storage equipment to truly reproduce the impact of different load conditions and environmental variables on system performance. In the test bench, a high-frequency data acquisition module is used to record the system operation status in real time, including key parameters such as voltage, current, temperature and light intensity, providing reliable measured data support for model verification.

In the development of the intelligent control part, this study implements a control algorithm based on DQN-LSTM and embeds it into the experimental test bench for real-time verification. To adapt the intelligent control algorithm to the actual system, the parameters are optimized according to the operating characteristics of

the test bench, and the stability and efficiency of the control strategy are determined through multiple rounds of experiments. At the same time, the experimental results are compared and analyzed with the simulation data to verify the effectiveness and superiority of the proposed method in practical applications, ensuring the integrity of the research from theory to experiment to practical application and enhancing the persuasiveness and practicality of the research results.

A view of the PV SC integrated station with all measurement instruments and data acquisition systems is shown in Figure 4.

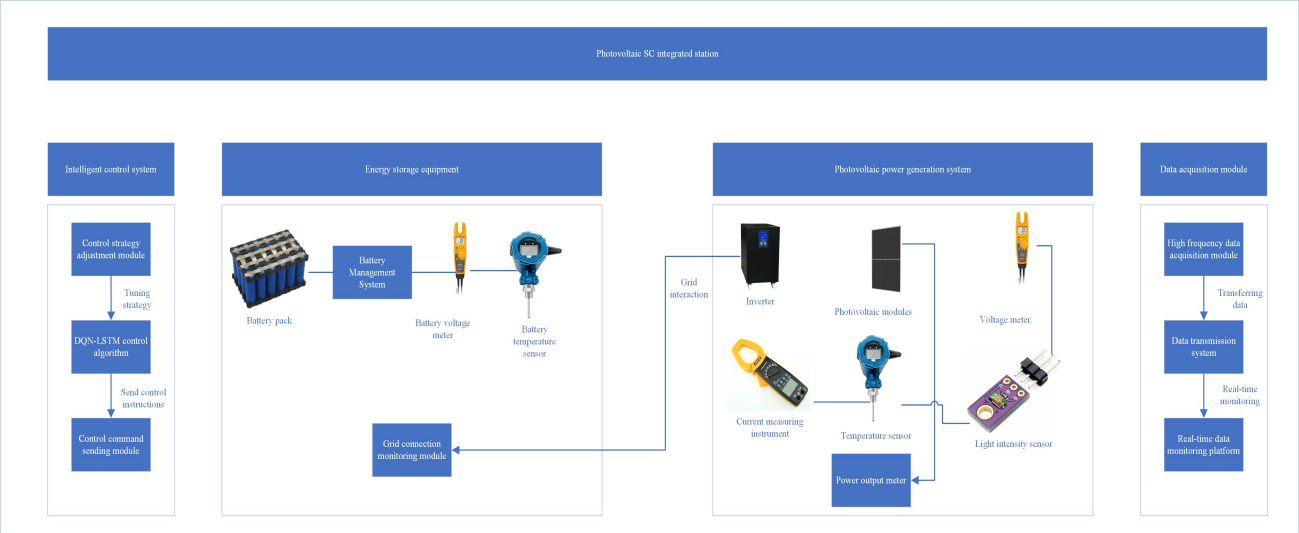

Figure 4. View of the photovoltaic SC integrated station and all measuring instruments and data acquisition systems

In Figure 4, the view of the photovoltaic SC integrated station and all measuring instruments and data acquisition systems shows the overall architecture of the photovoltaic storage and charging integrated system and the interactive relationship between key components. The system uses integrated photovoltaic power generation, energy storage equipment and intelligent control modules to monitor and adjust the operating status of the system in real time. The photovoltaic power generation system collects power output, light intensity and environmental data through photovoltaic modules, inverters, voltage and current meters, temperature sensors and other equipment. The energy storage system uses battery packs, battery management systems and related measuring equipment to monitor the charging and discharging process of the battery. The data acquisition module is responsible for the collection and transmission of high-frequency real-time data, and the data is analyzed and displayed through the monitoring platform. The intelligent control system is dynamically adjusted based on the DQN-LSTM algorithm to optimize the grid-connected/off-grid mode switching strategy of the photovoltaic storage and charging system and improve the system's operating efficiency and stability. The integration of the entire system enables the experimental test bench to effectively verify the intelligent control algorithm's performance in a real environment and provide reliable data support for practical applications.

The high-frequency data acquisition module is an important part of the photovoltaic storage and charging integrated system, which includes a data acquisition card, photovoltaic voltage and current sensors, temperature sensors, light intensity sensors, data storage and transmission modules, system control modules, and power analyzers. The design specifications and parameters of the high-frequency data acquisition module are shown in Table 1.

Table 1 shows the specifications and parameters of each component in the high-frequency data acquisition module. For the data acquisition card, the design specifications include the sampling frequency, number of input channels, accuracy, input range, and parameters including sampling accuracy and maximum sampling speed.

Table 1. Design specifications and parameters of the high-frequency data acquisition module

Data Acquisition Card	Sampling frequency	Number of input channels	Accuracy	Input range	Sampling accuracy	Maximum sampling speed
	1000 Hz	16 channels	16 bits	0-10 V voltage input, 0-20 A current input	±0.1%	1 MS/s
Photovoltaic voltage	Voltage measurement range	Current measurement range	Response time	Accuracy	Noise	Rated operating temperature
	0-600 V	0-20 A	Less than 5 ms	±0.5%	≤1 mV	-20°C to +60°C
Temperature sensor	Temperature measurement range	Response time	Accuracy	Resolution	Analog signal output	Digital signal output
	-40°C to +85°C	Less than 500 ms	±0.1°C	0.01°C	0-5 V	I2C, SPI
Light intensity sensor	Light intensity range	Response time	Accuracy	Resolution	Analog output interface	
	0-2000 W/m²	Less than 200 ms	±3%	1 W/m²	0-10 V	
Data storage and transmission module	Storage capacity	Transmission protocol	Data interface	Storage capacity	Transmission rate	
	24 hours	Ethernet or Wi-Fi	Supports USB, RS-232, RS-485	≥16 GB	At least 1 Gbps	
System Control Module	I/O interface	Processor frequency	Memory capacity		System response time	
	Supports multiple input and output interfaces (GPIO, PWM, SPI, I2C)	≥1 GHz	≥4 GB		Less than 1 ms	
Power Analyzer	Power measurement range	Accuracy	Measurement accuracy	Response time	Analog output interface	
	0-100 kW	±0.1%	±0.1%	Less than 1 m	0-10 V	

B. Experimental Data and Preprocessing

The experimental data in this paper comes from the PV SC integrated station actually deployed in a certain area. The data is collected in real time every 10 minutes by the monitoring system of the station from January to June 2023. The data includes PVPG (PV power generation), energy storage battery charging and discharging power, grid power load, user load demand, energy storage battery power, temperature, humidity, light intensity, etc. In the experiment, 180 days of operation data, about 25,920 sets of data records, are collected. Some experimental data are shown in Table 2.

Table 2. Some experimental data

Number of groups	PV power generation (kW)	Energy storage battery charging and discharging power (kW)	Grid power load (kW)	User load demand (kW)	Energy storage battery power (kWh)	Temperature (°C)	Humidity (%)	Light intensity (W/m²)
1	120	40	80	100	300	28	65	900
2	130	35	75	110	295	29	60	950
3	140	45	85	120	310	30	70	1000
4	110	30	90	90	280	27	55	850
5	95	20	100	85	270	26	80	800
6	100	50	95	95	320	25	75	880
7	150	60	70	115	350	32	68	1100
8	80	15	105	75	260	24	60	700
9	125	55	80	100	330	29	72	950
10	135	40	90	110	315	30	68	980

Table 2 shows 10 sets of data in 180 days, including PVPG, energy storage battery charging and discharging power, grid power load, user load demand, energy storage battery power and some environmental information.

Preprocessing

(1) Data cleaning

For missing value data, linear interpolation is used to fill in the data. For continuous data, the linear relationship between the previous and next data is used to fill missing values to ensure smooth data transition, while for discrete data, the nearest neighbor interpolation method is used to fill in the missing values.

(2) Data normalization

The dimensions and numerical ranges are quite different. This paper uses the Min-Max normalization method to map the value of each feature to the interval [0, 1] to eliminate the dimensional differences between different features.

C. Experimental Design

Experimental Objectives:

(1) Optimizing the switching strategy can enable the system of the PV SC integrated station to operate efficiently and stably under different load demands and environmental conditions, maximize energy utilization and reduce energy loss.

(2) It can ensure that the intelligent control model can respond in real time and make accurate automatic switching decisions, thereby improving the real-time and flexibility of the system.

Based on the above experimental data, the experimental steps are as follows:

① The collected experimental data can be cleaned and smoothed first, and normalized using Min-Max.

② The experiment constructs a PV SC integrated station model, which is divided into PVPG, energy storage system, power grid model and load demand model, and designs the objective function and formulates the constraints.

③ The study uses the LSTM model to predict the load demand and PVPG of the PV SC integrated station in the future, and inputs it into the DQN model.

④ Based on the prediction results and the current environmental status, the DQN model makes intelligent grid-connected or off-grid switching decisions for the integrated PV SC station.

⑤ The automatic switching decision performance of the fusion model DQN-LSTM in the integrated PV SC station GC/OG mode can be statistically analyzed.

To verify the effectiveness of the proposed method, a photovoltaic integrated power station is used in a medium-sized industrial park with a load demand of 200 kW-500 kW and a photovoltaic power of 100 kW-250 kW. The capacity of the energy storage battery is generally designed to be 1.5-2 times the photovoltaic power generation power, and the energy storage battery capacity is designed to be 150 kWh to 500 kWh.

The basic system structure of the photovoltaic integrated power station includes a photovoltaic power generation system, an energy storage system, a control strategy and decision system, and a grid/load connection module. It is assumed that the system scale is further expanded to increase the photovoltaic power generation capacity to 1 MW to 5 MW, or to expand to a larger industrial area or a power station in multiple regions. In that case, the method proposed in this paper is still applicable, but there are some limitations.

(1) As the scale increases, the load demand, photovoltaic power generation, and energy storage capacity increase significantly, resulting in an increase in the computational complexity of the DQN and LSTM models. It is necessary to adopt a more efficient optimization algorithm or distributed computing method to maintain the real-time response capability of the system.

(2) When the scale is expanded, the system's real-time response and control decision-making delay can increase, so combining edge computing or cloud computing technology is necessary to further optimize the system's response time and computing power.

(3) Larger-scale systems have more complex dynamic changes, and the platform needs to retrain and adjust the DQN and LSTM models to ensure the accuracy and effectiveness of decisions.

The experimental hyperparameter settings are shown in Table 3.

Table 3. Hyperparameters

Parameters	Value	Parameters	Value
Learning rate	0.001	Number of hidden layer units	128
Discount factor	0.9	Time step	10
Experience replay pool size	5000	Optimizer	Adam
Batch size	64	Number of training rounds	100

In the experimental application, this paper encounters some challenges, including incomplete and unbalanced data sets, making it difficult for the model to obtain effective learning results during training. The actual data of photovoltaic power generation and energy storage systems are greatly affected by environmental factors, resulting in data volatility and uncertainty, further increasing the complexity of model prediction. This paper preprocesses the data and uses data enhancement technology to balance the data set by supplementing and expanding samples to improve the generalization ability of the model. The hyperparameters in the model training process are optimized, and the cross-validation method is combined to avoid overfitting to ensure that the model can maintain good performance under different conditions.

During the training process, the DQN-LSTM model's convergence speed is slow. Especially when facing complex power grid scheduling and load demand changes, the amount of calculation in the training process is large. This paper adopts the model parallelization method to distribute the computing tasks to multiple processing units for parallel computing, which greatly accelerates the training speed. At the same time, in terms of algorithm optimization, the experience replay mechanism and target network update strategy are adopted to effectively improve the training stability and reduce the fluctuations in the training process.

D. Experimental Results

1) Grid-Connected/Off-Grid Switching Accuracy, Precision and Efficiency of Different Models

To evaluate the automatic switching decision-making performance of the integrated PV SC station GC/OG mode, the GC/OG switching accuracy, precision and efficiency is used in the experiment to analyze the automatic decision-making performance. The results are shown in Figure 5. In Figure 5, the comparison models include TD3-LSTM (Twin Delayed Deep Deterministic policy gradient-Long Short-Term Memory), A3C-LSTM (Asynchronous Advantage Actor-Critic-Long Short-Term Memory), DQN, and PID.

Switching accuracy refers to the proportion of the model correctly switching to the target mode (grid-connected or off-grid). The model's prediction of when to switch to the grid or off-grid matches the actual demand. High accuracy indicates that the model can accurately identify and execute the correct mode switch. Switching accuracy measures the accuracy of the model's switching decision. It is mainly used to evaluate the deviation between the actual correct switch (grid-connected or off-grid) and the predicted decision result in the switching decision made by the model. It focuses on the number of wrong switches of the model. If the model predicts that the grid should be switched, but it should actually be off-grid, then this wrong switch will affect the accuracy. Switching efficiency refers to the amount of time or resources consumed by the model when switching between grid-connected and off-grid modes. A high-efficiency model can make decisions and execute the switch in a shorter time, reducing the response delay of the system.

Accuracy focuses on the correctness of the model's switching decision, that is, whether the correct grid-connected or off-grid mode selection is made. Precision pays more attention to the proportion of wrong switches, evaluating the "wrong" situation of the model when executing the switching decision. Efficiency reflects the resource consumption and time efficiency of the model when executing the decision. Switching efficiency is quantified by analyzing the time and resources consumed by each model when performing a switch. Switching precision is quantified by calculating the ratio of correct switches predicted by the model to all predicted switches, and switching accuracy is quantified by comparing the correct switching ratios of different models.

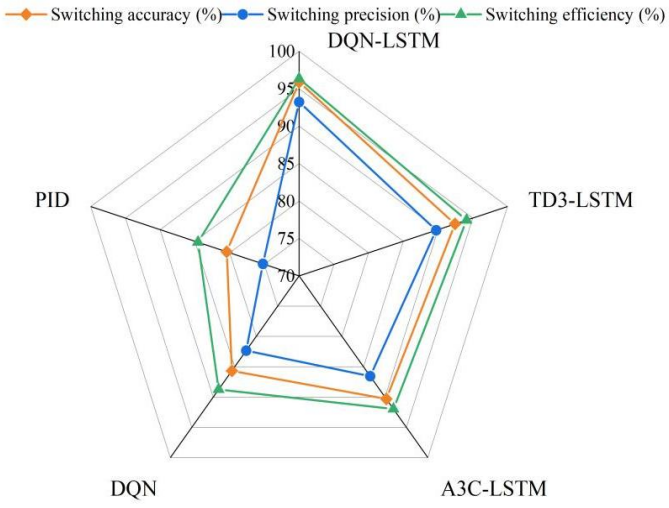

Figure 5. GC/OG switching accuracy, precision and efficiency of different models

In terms of switching precision, DQN-LSTM reaches 93.22%, and A3C-LSTM reaches 86.56%. In contrast DQN and PID have precision rates of only 82.33% and 75.21%, respectively. In terms of switching efficiency, DQN-LSTM performs best, reaching 96.34%, while PID only reaches 84.56%. In summary, the DQN-LSTM model achieves the best performance in automatic switching decision-making for the GC/OG mode integrated PV SC station. DQN-LSTM uses the Q-learning algorithm in deep reinforcement learning to dynamically adjust the decision-making strategy so that it can better adapt to changes in complex environments. The PID model uses simple rule control, which is difficult to cope with complex decision-making needs and has a low accuracy rate.

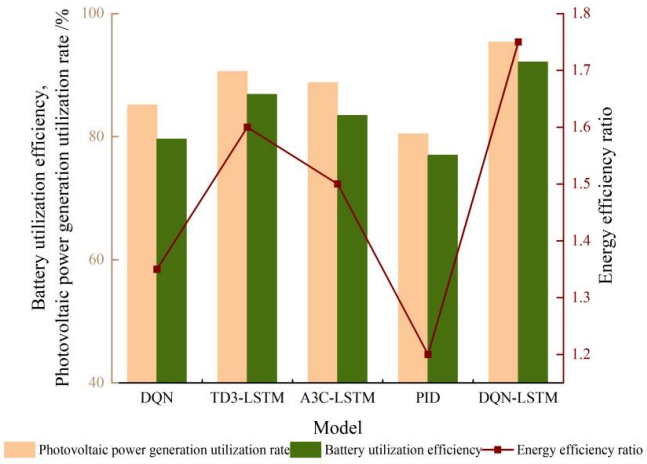

Figure 6. Analysis of energy management effect

2) *Energy Management Effects*

Energy management is crucial in a PV SC integrated station. A good switching strategy can often reduce energy consumption and improve utilization. The experiment counts the PVPG utilization rate and battery utilization rate, and the energy efficiency ratio is used to measure the overall energy utilization efficiency. The energy management effect analysis is shown in Figure 6. The higher the energy efficiency ratio, the more useful output the system can produce under unit energy input.

In Figure 6, from the perspective of energy efficiency ratio, the DQN-LSTM model performs best, with an energy efficiency ratio of 1.75, which is 0.55 higher than PID. The energy efficiency ratios of TD3-LSTM and A3C-LSTM are 1.6 and 1.5 respectively. The energy efficiency ratios of DQN and PID are 1.35 and 1.2 respectively, and the energy efficiency management is relatively inefficient.

In terms of PVPG utilization and battery utilization, the PVPG utilization and battery utilization efficiency of the DQN-LSTM model reach 95.35% and 92.12% respectively, with the highest utilization rate. The PVPG utilization rate of DQN is only 85.12%, and the battery utilization efficiency is 79.61%. PID performs the worst, with a PVPG utilization rate of only 80.45% and a battery utilization efficiency of only 76.98%. DQN-LSTM uses deep reinforcement learning to achieve more accurate scheduling and switching, which can maximize the use of PVPG and energy storage systems.

3) *Comparison of Load Demand and PVPG Prediction Performance*

In Figure 7, the comparison models include GRU (Gated Recurrent Unit), ARIMA (Autoregressive Integrated Moving Average model), RF (Random Forest), and KNN (k-nearest neighbor).

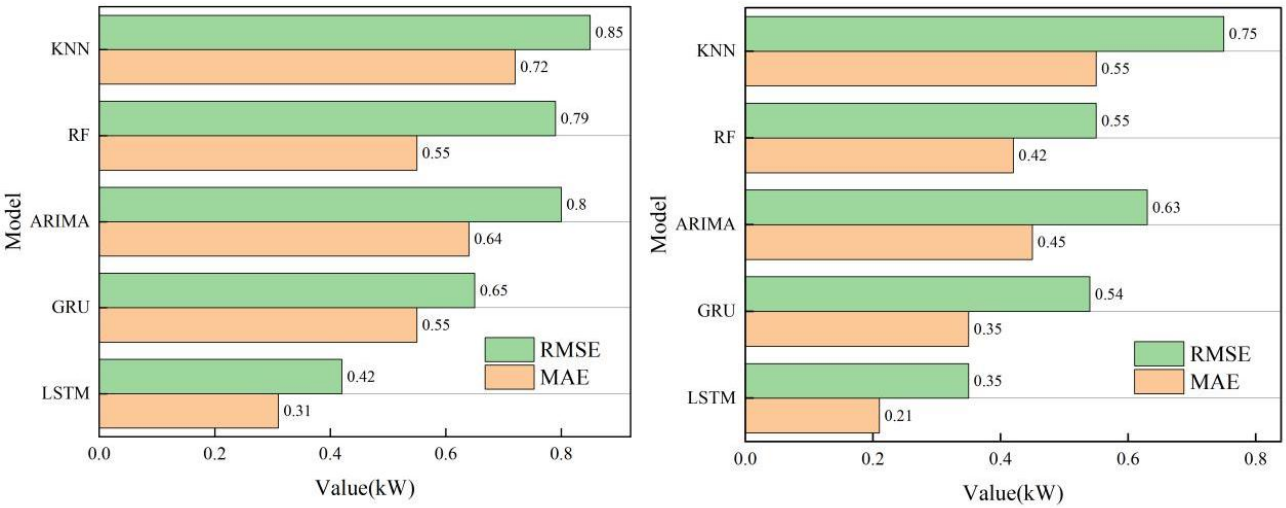

Figure 7. Comparison of load demand and PVPG prediction performance. Figure 7 (a) Load demand prediction performance, Figure 7 (b) PVPG prediction performance.

In Figure 7, Figure 7 (a) shows the load demand prediction performance, and Figure 7 (b) shows the PVPG prediction performance. In Figure 7(a), the LSTM model performs best, with a MAE (Mean Absolute Error)

of only 0.31 kW and an RMSE (Root Mean Square Error) of only 0.42 kW. The MAE of the GRU model is 0.55 kW and the RMSE is 0.65 kW, which is worse than the LSTM. The KNN has the highest MAE of 0.72 kW and the RMSE of 0.85 kW, with the largest error.

In Figure 7 (b), the LSTM performs well, with an MAE of 0.21 kW and an RMSE of 0.35 kW. The MAE of KNN is 0.55 kW and the RMSE is 0.75 kW. In summary, LSTM has a high accuracy in load demand and PVPG prediction due to its powerful time series modeling ability, and can make more accurate predictions of load demand and PVPG.

4) Real-time Performance of Intelligent Decision-Making

To further explore the real-time decision-making of the integrated PV SC station, its decision response time, training time, training speed, and parameter quantity are statistically analyzed. The results are shown in Figure 8.

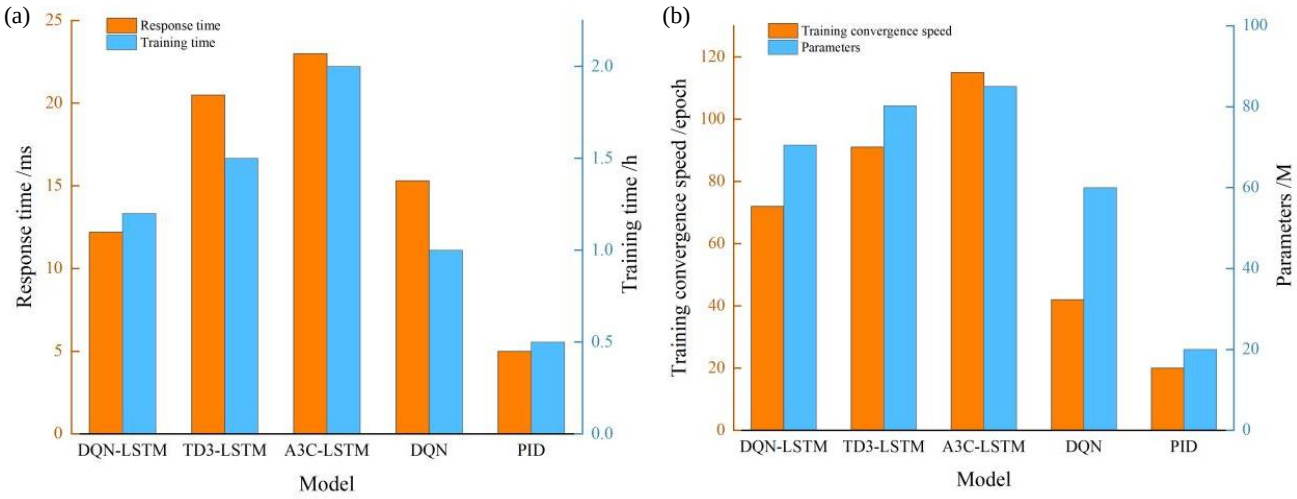

Figure 8. Real-time performance of intelligent decision-making. Figure 8 (a) Decision response time and training time, Figure 8(b) Training speed and parameter amount.

In Figure 8, Figure 8(a) represents the decision response time and training time, and Figure 8(b) represents the training speed and parameter amount. In Figure 8 (a), the PID model performs best in decision response time, which is only 5.0 ms. The A3C-LSTM model has the longest response time, up to 23.0 ms. The DQN-LSTM model reaches 12.2 ms, which shows that it has a certain degree of real-time performance. In terms of training time, the DQN-LSTM model training time is only 1.2 hours, while the TD3-LSTM model and the A3C-LSTM model reach 1.5 hours and 2 hours respectively.

In Figure 8 (b), from the perspective of training convergence speed, DQN-LSTM converges faster, and the convergence speed of DQN is only 42 epochs, which is slightly slower than traditional PID control. The training speed of TD3-LSTM and other models is slower, among which the TD3-LSTM model reaches 91 epochs. In terms of parameter quantity, the PID model has the least number of parameters, which is only 20M. The number of parameters of DQN-LSTM is 70.5M, while the number of parameters of TD3-LSTM and A3C-LSTM is 80.2M and 85M respectively. In summary, the DQN-LSTM model achieves good real-time decision-making and meets actual needs.

5) Economic Benefits and Energy-Saving Effects

The PV SC integrated station is characterized by energy saving and high efficiency. In order to explore the performance results of the DQN-LSTM experimental method applied to the PV SC integrated station, the economic benefits and energy saving effects are analyzed by electricity cost, maintenance cost, and investment payback period. The results of the economic benefit and energy saving effect analysis are shown in Figure 9.

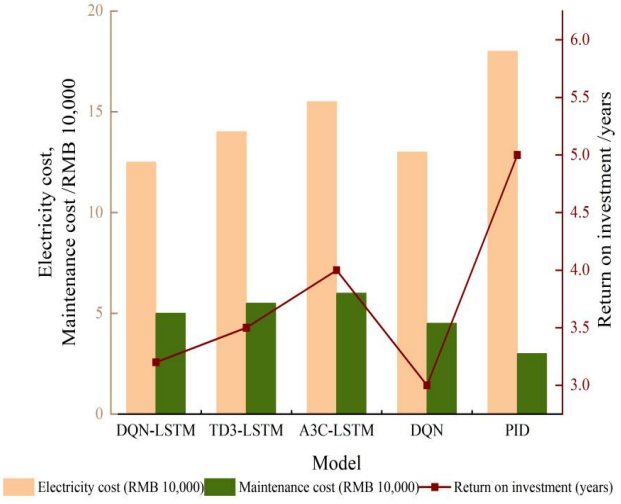

Figure 9. Economic benefits and energy-saving effects

In Figure 9, the DQN-LSTM model performs best in terms of electricity cost, with an electricity cost of 125,000 yuan, while the electricity cost of TD3-LSTM is 140,000 yuan and that of DQN is 130,000 yuan. The PID model has the highest electricity cost, which is 180,000 yuan. In terms of maintenance cost, PID has the lowest maintenance cost, which is only 30,000 yuan, while the maintenance cost of DQN-LSTM is 50,000 yuan. It can be found that the maintenance cost of deep learning methods can increase, and it requires the maintenance of more complex computing models and systems.

In terms of the payback period, DQN-LSTM has a shorter payback period of 3.2 years, indicating that it has better economic benefits in terms of energy saving. The payback period of DQN is 3 years. The payback periods of TD3-LSTM and A3C-LSTM are 3.5 years and 4 years, respectively, and PID has the longest payback period of up to 5 years. Overall, the DQN-LSTM model has a shorter payback period in terms of economic benefits and energy saving compared to the traditional PID control method, and the integrated PV SC station is in line with the green and low-carbon development of society.

The theoretical research in this paper reveals the dynamic interaction mechanism between smart grids, renewable energy stations and energy storage systems, and provides theoretical support for optimization control in real-time environments. This study explores how smart grids can achieve efficient utilization of power resources and balance supply and demand by coordinating distributed energy scheduling and energy storage system management under uncertain load demand and variable energy input. The theoretical model provides a framework for improving real-time monitoring, prediction, and response capabilities, which can guide the design of optimization algorithms in practical environments and promote the stability, reliability, and sustainable development of smart grids.

6) Comparison with Other Literature

The results of comparison with other literature are shown in Table 4.

Table 4. Comparison results with other literature

References	Switching accuracy (%)	Switching efficiency (%)	Switching time (s)
DQN-LSTM	95.87	96.34	0.01
EP-ANFIS [9]	92.45	91.78	0.78
Adaptive fuzzy PID [10]	83.62	82.95	0.56
NMC [11]	90.13	89.34	0.42
MPSO [13]	93.76	94.21	0.15

Table 4 shows that DQN-LSTM has a switching accuracy of 95.87% and a switching efficiency of 96.34%, which are significantly better than other literature methods, and the switching time is only 0.01s. The accuracy and efficiency of EP-ANFIS and NMC are good, but the switching time is long. The adaptive fuzzy PID method is simple, but its accuracy and efficiency are only 83.62% and 82.95% respectively, which are far lower than other methods. The performance of MPSO is relatively balanced, with a switching accuracy of 93.76%, a switching efficiency of 94.21%, and a switching time of 0.15s, which is suitable for scenarios with medium real-time requirements. In summary, DQN-LSTM has significant advantages in the comprehensive performance of high accuracy, high efficiency and extremely low switching time, demonstrating the potential of theoretical research and practical application.

4. Experimental Discussion

In the experiment, the DQN-LSTM model performs well in multiple performance indicators, among which the accuracy, precision and efficiency of GC/OG switching exceeded other models. In terms of energy management, the DQN-LSTM model is characterized by the highest PVPG utilization rate and battery utilization efficiency, which significantly improves the system's energy efficiency, and is significantly higher than that of PID. In terms of load demand and PVPG prediction, the LSTM model performs well, showing its strong ability in time series prediction tasks. During training, the DQN-LSTM model has a shorter training time and faster convergence speed. DQN-LSTM combines DQN and LSTM and can flexibly adapt to complex environmental changes by dynamically adjusting decision-making strategies, achieving more precise control and more efficient energy management.

This study introduces advanced deep learning technology, deep reinforcement learning and LSTM, to optimize the integrated PV SC station's energy management and decision-making process. The DQN-LSTM model has shown obvious advantages in multiple dimensions, improving the GC/OG switching accuracy of the system, enhancing energy utilization, reducing electricity costs, and shortening the investment payback period. The research is of great significance to promoting the intelligent management of integrated PV SC station. By optimizing switching decisions and energy scheduling, it

can achieve more efficient energy utilization, thereby promoting the application of green and low-carbon energy. The research results show that the intelligent decision-making system based on deep reinforcement learning has great potential in improving system operation efficiency, energy conservation and emission reduction. It can be extended to a wider range of energy management systems, which can help promote technological progress and application in the fields of smart grids and renewable energy.

5. Conclusions

This paper adopts for the first time an intelligent control strategy combining DQN with the time series prediction LSTM model for automatic switching of the grid-connected/off-grid mode of integrated photovoltaic storage and charging stations. It combines LSTM to predict future load and PVPG and inputs DQN for decision optimization, which effectively improves the system's switching accuracy, energy efficiency ratio and overall energy management efficiency. This study has made some achievements, but there are still some shortcomings. The responsiveness of the experimental model needs to be further optimized, and the computational complexity is high when deployed on a large scale. Future work and prospects are as follows:

(1) Design customized energy scheduling strategies based on the climate characteristics and user load characteristics of different geographical regions to enhance the regional adaptability and accuracy of the model.

(2) Combine distributed edge computing and cloud computing technologies to distribute computing tasks between site edge devices and central servers, reduce computing delays and improve system scalability and stability.

(3) Explore strategies for multi-energy coordinated scheduling, such as wind and solar complementarity, hydrogen energy storage, etc., to further improve the green energy utilization efficiency of the system and promote the innovative application of sustainable energy.

Acknowledgment

None

Data Availability Statement

The data that support the findings of this study are available from the corresponding author, upon reasonable request.

Funding

None

Author Contribution

Han Fu: Conceived and designed the research, conducted experiments, and analyzed data. Drafted and revised the manuscript critically for important intellectual content.

Xiaoyu Liu: Contributed to the acquisition, analysis, and interpretation of data. Provided substantial intellectual input during the drafting and revision of the manuscript.

Xiaoming Chen: Participated in the conception and design of the study.

Yuanqi Ni, Hong Zheng: Played a key role in data interpretation and manuscript preparation.

All authors have read and approved the final version of the manuscript.

Conflicts of Interest

The authors declare that they have no financial conflicts of interest.

References

[1] E.T. Sayed, A.G. Olabi, A.H. Alami, A. Radwan, A. Mdallal, et al. Renewable energy and energy storage systems. Energies. 2023, 16(3), 1415-1440. DOI: 10.3390/en16031415

[2] M.M. Gulzar, A. Iqbal, D. Sibtain, M. Khalid. An innovative converterless solar PV control strategy for a grid connected hybrid PV/wind/fuel-cell system coupled with battery energy storage. IEEE Access. 2023, 11, 23245-23259. DOI: 10.1109/ACCESS.2023.3252891

[3] P. Barman, L. Dutta, S. Bordoloi, A. Kalita, P. Buragohain, et al. Renewable energy integration with electric vehicle technology, A review of the existing smart charging approaches. Renewable and Sustainable Energy Reviews. 2023, 183(1), 1-15. DOI: 10.1016/j.rser.2023.113518

[4] A. Mohammed, O. Saif, M. Abo-Adma, A. Fahmy, R. Elazab. Strategies and sustainability in fast charging station deployment for electric vehicles. Scientific Reports. 2024, 14(1), 283-201. DOI: 10.1038/s41598-023-50825-7

[5] S.S.G. Acharige, M.E. Haque, M.T. Arif, N. Hosseinzadeh, K.N. Hasan, et al. Review of electric vehicle charging technologies, standards, architectures, and converter configurations. IEEE Access. 2023, 11(1), 41218-41255. DOI: 10.1109/ACCESS.2023.3267164

[6] M. Yao, D.N. Da, X.C. Lu, Y.H. Wang. A review of capacity allocation and control strategies for electric vehicle charging stations with integrated photovoltaic and energy storage systems. World Electric Vehicle Journal. 2024, 15(3), 101-128. DOI: 10.3390/wevj15030101

[7] K.Y. Wu, T.C. Tai, B.H. Li, C.C. Kuo. Dynamic Energy Management Strategy of a Solar-and-Energy Storage-Integrated Smart Charging Station. Applied Sciences. 2024, 14(3), 1188-1204. DOI: 10.3390/app14031188

[8] J. Hmad, A. Houari, A.E.M. Bouzid , A. Saim, H. Trabelsi. A review on mode transition strategies between grid-connected and standalone operation of voltage source inverters-based microgrids. Energies. 2023, 16(13),

5062-5102. DOI: 10.3390/en16135062
[9] S.V. Karemore, E.V. Kumar. Design of efficient storage unit and EP-ANFIS controller for on-grid and off-grid connected PV-WT system. Periodica Polytechnica Electrical Engineering and Computer Science. 2022, 66(4), 336-349. DOI: 10.3311/PPee.20364
[10] V. Gopu, M.S. Nagaraj. Adaptive fuzzy PID integrated renewable power management system for off grid and on grid conditions. International Journal of Power Electronics and Drive Systems (IJPEDS). 2024, 15(4), 2580-2590. DOI: 10.11591/ijpeds.v15.i4.pp2580-2590
[11] H.Y. Qing, C.J. Zhang, J.Y. Xu, S.L. Zeng, X.Q. Guo. A Nonlinear Multimode Controller for Seamless off-Grid of Energy Storage Inverter Under Unintentional Islanding. IEEE Transactions on Industrial Electronics. 2023, 70(12), 12354-12364. DOI: 10.1109/TIE.2022.3232639
[12] M. Kampik, M. Fice, A. Jurkiewicz. Adaptation of a cogenerator with induction generator to an on/off-grid operation using a power electronic system. Applied Sciences. 2023, 13(10), 5866-5889. DOI: 10.3390/app13105866
[13] V. Perumal, S.K. Kannan, C.R. Balamurugan. Grid Mode Selection Scheme based on a Novel Fractional Order Proportional Resonant Controller for Hybrid Renewable Energy Resources. Electric Power Components and Systems. 2023, 51(09), 1-20. DOI: 10.1080/15325008.2023.2202674
[14] Y. Xu, W.J. Gao, Y.X. Li. Cost-Effective Optimization of the Grid-Connected Residential Photovoltaic Battery System Based on Reinforcement Learning. Human-Centric Computing and Information Sciences. 2024, 14(2), 1-19. DOI: 10.22967/HCIS.2024.14.002
[15] X.K. Ding, J.W. Cao. Deep and Reinforcement Learning in Virtual Synchronous Generator, A Comprehensive Review. Energies. 2024, 17(11), 2620-2639. DOI: 10.3390/en17112620
[16] B. Zhang, W.H. Hu, X. Xu, T. Li, Z.Y. Zhang, et al. Physical-model-free intelligent energy management for a grid-connected hybrid wind-microturbine-PV-EV energy system via deep reinforcement learning approach. Renewable Energy. 2022, 200(1), 433-448. DOI: 10.1016/j.renene.2022.09.125
[17] M. Nicola, C.I. Nicola, D. Selișteanu. Improvement of the control of a grid connected photovoltaic system based on synergetic and sliding mode controllers using a reinforcement learning deep deterministic policy gradient agent. Energies. 2022, 15(7), 2392-2423. DOI: 10.3390/en15072392
[18] J.J. Qi, L. Lei, K. Zheng, S.X. Yang, X.M. Shen. Optimal scheduling in IoT-driven smart isolated microgrids based on deep reinforcement learning. IEEE Internet of Things Journal. 2023, 10(18), 16284-16299. DOI: 10.48550/arXiv.2305.00127
[19] F. Mohammad, D.K. Kang, M.A. Ahmed, Y.C. Kim. Energy demand load forecasting for electric vehicle charging stations network based on convlstm and biconvlstm architectures. IEEE Access. 2023, 11(1), 67350-67369. DOI: 10.1109/ACCESS.2023.3274657
[20] C.Y. Yang, H. Zhou, X.M. Chen, J.J. Huang. Demand Time Series Prediction of Stacked Long Short-Term Memory Electric Vehicle Charging Stations Based on Fused Attention Mechanism. Energies. 2024, 17(9), 2041-2056. DOI: 10.3390/en17092041
[21] P. Aduama, Z.B. Zhang, A.S. Al-Sumaiti. Multi-feature data fusion-based load forecasting of electric vehicle charging stations using a deep learning model. Energies. 2023, 16(3), 1309-1322. DOI: 10.3390/en16031309
[22] A. Avar, E. Ghanbari. Optimal integration and planning of PV and wind renewable energy sources into distribution networks using the hybrid model of analytical techniques and metaheuristic algorithms, A deep learning-based approach. Computers and Electrical Engineering. 2024, 117, 109280. DOI: 10.1016/j.compeleceng.2024.10928
[23] A.M. Abomazid, N.A. El-Taweel, H.E.Z. Farag. Optimal energy management of hydrogen energy facility using integrated battery energy storage and solar photovoltaic systems. IEEE Transactions on Sustainable Energy. 2022, 13(3), 1457-1468. DOI: 10.1109/TSTE.2022.3161891
[24] Y.J. Liu, L.N. Jian, Y.W. Jia. Energy management of green charging station integrated with photovoltaics and energy storage system based on electric vehicles classification. Energy Reports. 2023, 9(1), 1961-1973. DOI: 10.1016/j.egyr.2023.04.099
[25] P. Ray, C. Bhattacharjee, K.R. Dhenuvakonda. Swarm intelligence-based energy management of electric vehicle charging station integrated with renewable energy sources. International Journal of Energy Research. 2022, 46(15), 21598-21618. DOI: 10.1002/er.7601
[26] G. Krishna, R. Singh, A. Gehlot, S.V. Akram, N. Priyadarshi, et al. Digital technology implementation in battery-management systems for sustainable energy storage, Review, challenges, and recommendations. Electronics. 2022, 11(17), 2695-2718. DOI: 10.3390/electronics11172695
[27] K. Okay, S. Eray, A. Eray. Development of prototype battery management system for PV system. Renewable Energy. 2022, 181(1), 1294-1304. DOI: 10.1016/j.renene.2021.09.118
[28] A.F. Guven, E. Yücel. Sustainable energy integration and optimization in microgrids, enhancing efficiency with electric vehicle charging solutions. Electrical Engineering. 2024, 10(1), 1-33. DOI: 10.1007/s00202-024-02619-x
[29] H. Xiao, X.W. Pu, W. Pei, L. Ma, T.F. Ma. A novel energy management method for networked multi-energy microgrids based on improved DQN. IEEE Transactions on Smart Grid. 2023, 14(6), 4912-4926. DOI: 10.1109/TSG.2023.3261979
[30] X. Yang, P. Liu, F. Liu, Z.C. Liu, D.Q. Wang, J. Zhu, et al. A DOD-SOH balancing control method for dynamic reconfigurable battery systems based on DQN algorithm. Frontiers in Energy Research. 2023, 11(1), 1-13. DOI: 10.3389/fenrg.2023.1333147
[31] F. Yang, F. Gao, B.C. Liu, S. Ci. An adaptive control framework for dynamically reconfigurable battery systems based on deep reinforcement learning. IEEE Transactions on Industrial Electronics. 2022, 69(12), 12980-12987. DOI: 10.1109/TIE.2022.3142406
[32] K. Sivamayil, E. Rajasekar, B. Aljafari, S. Nikolovski, S. Vairavasundaram, et al. A systematic study on reinforcement learning based applications. Energies. 2023, 16(3), 1512-1534. DOI: 10.3390/en16031512
[33] S.W. Zhai, W.Y. Li, Z.Y. Qiu, X.Y. Zhang, S.X. Hou. An improved deep reinforcement learning method for dispatch optimization strategy of modern power systems. Entropy. 2023, 25(3), 546-568. DOI: 10.3390/e25030546
[34] E.M. Al-Ali, Y. Hajji, Y. Said, M. Hleili, A.M. Alanzi, et al. Solar energy production forecasting based on a hybrid CNN-LSTM-transformer model. Mathematics. 2023, 11(3), 676-684. DOI: 10.3390/math11030676
[35] D.K. Dhaked, S. Dadhich, D. Birla. Power output forecasting of solar photovoltaic plant using LSTM. Green Energy and Intelligent Transportation. 2023, 2(5), 1-9. DOI: 10.1016/j.geits.2023.100113
[36] S.S. Chandel, A. Gupta, R. Chandel, S. Tajjour. Review of deep learning techniques for power generation prediction of industrial solar photovoltaic plants. Solar Compass. 2023, 8(1), 1-12. DOI: 10.1016/j.solcom.2023.100061